

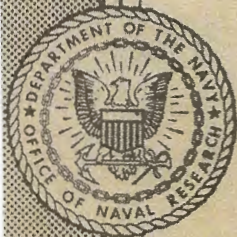
NRL REPORT 4197

# **GAMMA RADIATION FROM INTERACTION OF 14-MEV NEUTRONS WITH VARIOUS ELEMENTS**

V. E. Scherrer, R. B. Theus  
and W. R. Faust

Reactions Branch  
Radiation Division

June 22, 1953



**NAVAL RESEARCH LABORATORY**

**WASHINGTON, D.C.**

## ABSTRACT

Experiments have been performed to observe the gamma radiation produced by interaction of 14-Mev neutrons with various materials. These included carbon, oxygen, aluminum, iron, nickel, copper, cadmium, and lead. Generally the gamma spectrum of all elements appears to consist of a low energy continuum overlaid by a series of discrete lines or bands at higher energies. The square root of the total gamma-ray cross section is a linear function of  $A^{1/3}$  from carbon to cadmium.

## PROBLEM STATUS

This is a final report on one phase of the problem; work on the problem is continuing.

## AUTHORIZATION

NRL Problem H14-01  
RDB Project NR 464-010

Manuscript submitted June 12, 1953

## CONTENTS

Abstract	ii
Problem Status	ii
Authorization	ii
INTRODUCTION	1
DESCRIPTION OF THE EXPERIMENT	1
SPECTROMETER RESPONSE	2
RESULTS	4
Carbon	4
Oxygen	4
Aluminum	5
Iron	5
Nickel	5
Copper	5
Cadmium	5
Lead	5
DISCUSSION	6
ACKNOWLEDGMENTS	6

in conjunction with a twenty-channel pulse-height analyzer detected the gamma rays produced in the converter. The differential analyzer was gated only by coincidences between the alpha monitor and the spectrometer, thereby eliminating background counts from direct neutrons on the crystal as well as radiation scattered off the walls of the room. The amplifier discriminator in the alpha channel was set to eliminate low-level noise and counts from the  $D(d,n)He^3$  reaction and electrons. Scalers were placed at all points in the system that gave useful information.

Figure 3 shows typical calibration curves with the 4.45-Mev line of Po-Be and the two gamma lines of  $Co^{60}$ . These curves, after correction for the statistics of the 5819 photomultiplier tube and the finite channel width of the discriminator, resemble the theoretical response due to scattering and absorption of the gamma rays in the crystal.

## SPECTROMETER RESPONSE

The pulse-height distribution produced by a particular spectrum of gamma rays incident upon a crystal spectrometer can always be formulated in terms of the incident spectrum and the various parameters of the system. It is generally difficult to invert the resulting integral equation for the pulse-height distribution and to obtain thereby the energy spectrum of the incident gamma rays. However, this can be done for various simple cases which are good approximations to the particular cases considered herein.

The gamma rays generated by 14-Mev neutrons in the converter (Figure 4) produce a pulse-height distribution in the spectrometer. If  $d\sigma(E')/dE'$  is the differential cross section (barns/Mev) for the production of gamma rays of energy  $E'$ , then the number of gamma rays produced in a volume  $W_0 dh dl$  at a distance  $l$  from the front surface of the converter is:

$$\frac{N_\alpha}{h_0} AN \frac{d\sigma}{dE'} 10^{-24} dE' dh dl \quad (1)$$

where  $A$  is the attenuation of the neutron beam in the converter and  $N_\alpha$  is the number of neutrons incident upon the area  $W_0 h_0$  of the front surface of the converter; these and only these neutrons are in coincidence with the alpha monitor.

Let  $K(E, E')$  be the relative probability of finding a pulse whose height lies in the interval between  $E$  and  $E + dE$  whenever a gamma ray of energy  $E'$  produces a pulse in the spectrometer. Then the pulse-height distribution due to the gamma rays originating in  $W_0 dh dl$  is:

$$\frac{N_\alpha}{h_0} \frac{\Omega}{4\pi} AN 10^{-24} \frac{d\sigma}{dE'} dE' dh dl K(E, E') e^{-\mu_1(E')t} \left[ 1 - e^{-\mu_2(E')D} \right] \quad (2)$$

where  $\Omega$  is the solid angle subtended by the detector at the converter and  $\mu_1(E')$  and  $\mu_2(E')$  are the absorption coefficients for gamma rays

# GAMMA RADIATION FROM INTERACTION OF 14-MEV NEUTRONS WITH VARIOUS ELEMENTS

## INTRODUCTION

Experiments have been performed to observe gamma radiation produced by interaction of 14-Mev neutrons with a variety of elements. Previous experiments<sup>1,2</sup> were carried out principally by use of absorption techniques. To obtain better resolution measurements have been made with a spectrometer consisting of a single crystal of NaI(Tl) in conjunction with a twenty-channel pulse-height analyzer. Despite rather poor spectrometer resolution, a somewhat more detailed picture of the gamma-ray spectrum has been obtained.

## DESCRIPTION OF THE EXPERIMENT

A 250-kilovolt Cockcroft-Walton accelerator<sup>3</sup> employing the  $T(d,n)He^4$  reaction was used as a source of 14-Mev neutrons,<sup>4</sup> which were allowed to fall upon a converter arranged as shown in Figure 1.

The converter and the accelerator monitor were so placed that whenever an alpha particle entered the monitor the corresponding neutron entered the converter. Converters used were approximately 0.75 inelastic neutron mean free paths long, and sufficiently wide enough to just cover the "coincidence neutron beam." On the average a gamma ray traveled about 0.25 mean free paths before leaving the converter and reaching the detector.

Pulse-height distributions were taken with the appropriate converter in and out of the coincidence neutron beam to obtain source and background data. Generally the source to background ratio was ten to one or greater with the exception of oxygen as noted later.

A block diagram of the electronic arrangement is shown in Figure 2. A single crystal of NaI(Tl) and a 5819 photomultiplier

<sup>1</sup>D. E. Lea, "Secondary Gamma Rays Excited by the Passage of Neutrons Through Matter," Proc. Roy. Soc. 150:637 (1935)

<sup>2</sup>Private Communication from J. H. Coon of LASL describing some of their unpublished work.

<sup>3</sup>T. A. Bergstrahl, K. L. Dunning, E. Durand, C. H. Ellison, H. K. Howerton, and W. Slavin, "A Portable 250-Kilovolt Accelerator," (to be published in Rev. Sci. Instr.)

<sup>4</sup>E. R. Graves, A. A. Rodrigues, M. Goldblatt, and D. I. Meyer, Rev. Sci. Instr. 20:579 (1949)

in conjunction with a twenty-channel pulse-height analyzer detected the gamma rays produced in the converter. The differential analyzer was gated only by coincidences between the alpha monitor and the spectrometer, thereby eliminating background counts from direct neutrons on the crystal as well as radiation scattered off the walls of the room. The amplifier discriminator in the alpha channel was set to eliminate low-level noise and counts from the  $D(d,n)He^3$  reaction and electrons. Scalars were placed at all points in the system that gave useful information.

Figure 3 shows typical calibration curves with the 4.45-Mev line of Po-Be and the two gamma lines of  $Co^{60}$ . These curves, after correction for the statistics of the 5819 photomultiplier tube and the finite channel width of the discriminator, resemble the theoretical response due to scattering and absorption of the gamma rays in the crystal.

## SPECTROMETER RESPONSE

The pulse-height distribution produced by a particular spectrum of gamma rays incident upon a crystal spectrometer can always be formulated in terms of the incident spectrum and the various parameters of the system. It is generally difficult to invert the resulting integral equation for the pulse-height distribution and to obtain thereby the energy spectrum of the incident gamma rays. However, this can be done for various simple cases which are good approximations to the particular cases considered herein.

The gamma rays generated by 14-Mev neutrons in the converter (Figure 4) produce a pulse-height distribution in the spectrometer. If  $d\sigma(E')/dE'$  is the differential cross section (barns/Mev) for the production of gamma rays of energy  $E'$ , then the number of gamma rays produced in a volume  $W_0 dh dl$  at a distance  $l$  from the front surface of the converter is:

$$\frac{N_\alpha}{h_0} A N \frac{d\sigma}{dE'} 10^{-24} dE' dh dl \quad (1)$$

where  $A$  is the attenuation of the neutron beam in the converter and  $N_\alpha$  is the number of neutrons incident upon the area  $W_0 h_0$  of the front surface of the converter; these and only these neutrons are in coincidence with the alpha monitor.

Let  $K(E, E')$  be the relative probability of finding a pulse whose height lies in the interval between  $E$  and  $E + dE$  whenever a gamma ray of energy  $E'$  produces a pulse in the spectrometer. Then the pulse-height distribution due to the gamma rays originating in  $W_0 dh dl$  is:

$$\frac{N_\alpha}{h_0} \frac{\Omega}{4\pi} A N 10^{-24} \frac{d\sigma}{dE'} dE' dh dl K(E, E') e^{-\mu_1(E')t} \left[ 1 - e^{-\mu_2(E')D} \right] \quad (2)$$

where  $\Omega$  is the solid angle subtended by the detector at the converter and  $\mu_1(E')$  and  $\mu_2(E')$  are the absorption coefficients for gamma rays

Numerical solutions for  $d\sigma(E_j)/dE_j$  were then obtained by use of an analog computer.

## RESULTS

The net counting data for the various elements was obtained by subtraction of source and background observations. Figures 5 to 20 show data so obtained for the various elements in which the pulse-height distribution is plotted in counts per Mev per neutron, aside from a numerical factor. The analyzed data is also presented for each element. It should be pointed out that the exact shape and maximum of the continua is not significant. The integral of the spectral distribution is meaningful and is essentially independent of the exact method of analyzing the spectral distribution.

### Carbon

The pulse-height distribution for a carbon converter is given in Figure 5. For comparison, the pulse-height distribution in counts per second per Mev obtained from a Po-Be source is also plotted. The similarity of these curves is due to the condition that the residual excited nucleus is  $C^{12}$  in both reactions. The 4.45-Mev gamma ray<sup>5</sup> which appears at a secondary electron energy of 3.43 Mev due to the loss of the two 0.51-Mev annihilation quanta is quite evident in both cases. Differences between the two curves are probably due to the higher excitation produced by 14-Mev neutrons on carbon as compared with the excitation of the residual nucleus in the reaction  $Be^9(\alpha, n)C^{12}$ .

An analysis of the pulse-height distribution is given in Figure 6. Here there appear to be gamma rays at 2.8, 4.45, 6.0, and 7.0 Mev. The cross section for each line is 0.036, 0.069, 0.002, and 0.002 barns respectively, and the total gamma-ray production cross section is 0.19 barns.

### Oxygen

In these experiments, liquid oxygen in a vacuum flask was placed in the "coincidence neutron" beam. Pulse-height distributions were taken with the flask full and empty to obtain source and background data. The resulting source to background ratio was about three to one. Pulse-height distributions, so obtained, are given in Figure 7 and the analyzed spectrum is given in Figure 8. Here there appear to be lines at 3.0, 3.8, and 5.2 Mev, having production cross sections of 0.086, 0.13, and 0.056 barns respectively. The total cross section for gamma production is estimated to be 0.52 barns.

<sup>5</sup>J. Terrell, Phys. Rev. 80: 1076 (1950)

Numerical solutions for  $d\sigma(E_j)/dE_j$  were then obtained by use of an analog computer.

## RESULTS

The net counting data for the various elements was obtained by subtraction of source and background observations. Figures 5 to 20 show data so obtained for the various elements in which the pulse-height distribution is plotted in counts per Mev per neutron, aside from a numerical factor. The analyzed data is also presented for each element. It should be pointed out that the exact shape and maximum of the continua is not significant. The integral of the spectral distribution is meaningful and is essentially independent of the exact method of analyzing the spectral distribution.

### Carbon

The pulse-height distribution for a carbon converter is given in Figure 5. For comparison, the pulse-height distribution in counts per second per Mev obtained from a Po-Be source is also plotted. The similarity of these curves is due to the condition that the residual excited nucleus is  $C^{12}$  in both reactions. The 4.45-Mev gamma ray<sup>5</sup> which appears at a secondary electron energy of 3.43 Mev due to the loss of the two 0.51-Mev annihilation quanta is quite evident in both cases. Differences between the two curves are probably due to the higher excitation produced by 14-Mev neutrons on carbon as compared with the excitation of the residual nucleus in the reaction  $Be^9(\alpha, n)C^{12}$ .

An analysis of the pulse-height distribution is given in Figure 6. Here there appear to be gamma rays at 2.8, 4.45, 6.0, and 7.0 Mev. The cross section for each line is 0.036, 0.069, 0.002, and 0.002 barns respectively, and the total gamma-ray production cross section is 0.19 barns.

### Oxygen

In these experiments, liquid oxygen in a vacuum flask was placed in the "coincidence neutron" beam. Pulse-height distributions were taken with the flask full and empty to obtain source and background data. The resulting source to background ratio was about three to one. Pulse-height distributions, so obtained, are given in Figure 7 and the analyzed spectrum is given in Figure 8. Here there appear to be lines at 3.0, 3.8, and 5.2 Mev, having production cross sections of 0.086, 0.13, and 0.056 barns respectively. The total cross section for gamma production is estimated to be 0.52 barns.

<sup>5</sup>J. Terrell, Phys. Rev. 80:1076 (1950)

### Aluminum

The pulse-height distribution obtained from an aluminum converter is given in Figure 9 and the analyzed spectrum in Figure 10. The total production cross section is 1.7 barns while the cross sections are 0.176, 0.024, and 0.054 barns for the 1.7, 4.5, and 5.4 Mev gamma rays respectively. A cross section of 0.3 millibarns is estimated for the region above 11 Mev.

### Iron

The pulse-height distribution obtained with iron<sup>6</sup> is given in Figure 11 and the analyzed spectrum in Figure 12. There appear to be lines at 3.3, 4.4, 5.8, 7.1, and 8.8 Mev, having production cross sections of 0.277, 0.19, 0.077, 0.07, and 0.026 barns, respectively. The total cross section is 4.6 barns.

### Nickel

The pulse-height distribution and the analyzed spectrum is given in Figures 13 and 14, respectively. Lines at gamma ray energies of 2.9, 5.3, 6.6, and 8 Mev have cross sections of 0.096, 0.02, and 0.032 barns, respectively, while the total production cross section is 6 barns.

### Copper

A copper converter produced the pulse-height distribution of Figure 15. An analysis of this distribution gave the results of Figure 16. The total production cross section is 6.3 barns and the apparent lines at 3.1 and 4.5 Mev have cross sections of 0.052 and 0.024 barns, respectively. A cross section of 7 millibarns is estimated for the region above 8 Mev.

### Cadmium

The cadmium pulse-height distribution and analyzed spectrum are given in Figures 17 and 18. The total production cross section is 12.8 barns. There appears to be no definite line structure present.

### Lead

Lead pulse-height distribution and analyzed spectrum are given in Figures 19 and 20. It is found that the total production cross section is about 4.2 barns while lines at 4.4 and 5.5 Mev have cross sections of 0.048 and 0.017 barns, respectively.

<sup>6</sup>V. E. Scherrer, et al., Phys. Rev. 89:1268 (1953)

## DISCUSSION

Probable errors in the counting data are represented by vertical lines on the pulse-height distributions. There are, however, other sources of errors present in the analysis that are more serious than the counting statistics. These errors arise from uncertainties in absorption and scattering of neutrons and gamma rays in converter and crystal as well as lack of knowledge of the precise response of the spectrometer at all energies. It is estimated that the minimum error in the total production cross sections is about  $\pm 25$  percent while that associated with the lines is about  $\pm 35$  percent. There may also be an error of about 0.2 Mev in energy assignment.

Total gamma-ray production cross sections are summarized in Figure 21, where  $\sqrt{\sigma_0/\pi}$  is plotted against  $A^{1/3}$  in which  $A$  is the total number of particles in the nucleus. For comparison the inelastic cross section as given by Phillips<sup>7</sup> is plotted in the same figure. It is somewhat unexpected that the gamma-ray cross section can be so simply represented over such a large range of  $A$ . It is presumed in the case of lead,  $(n, 2n)$  reactions reduce the energy available for gamma-ray production so that the cross section falls below the value expected from extrapolating the curve. Carbon and oxygen, on the other hand, have gamma-ray production cross sections below the inelastic cross section. Here it is likely that emission of charged particles may reduce the energy available for gamma production.

## ACKNOWLEDGMENTS

The authors wish to thank Dr. E. H. Krause for his interest and support and express their appreciation to Messrs. A. P. Flanick and B. A. Allison for aid in performing the experiments.

---

<sup>7</sup>D. D. Phillips, et al., Phys. Rev. 88:600 (1952)

\* \* \*

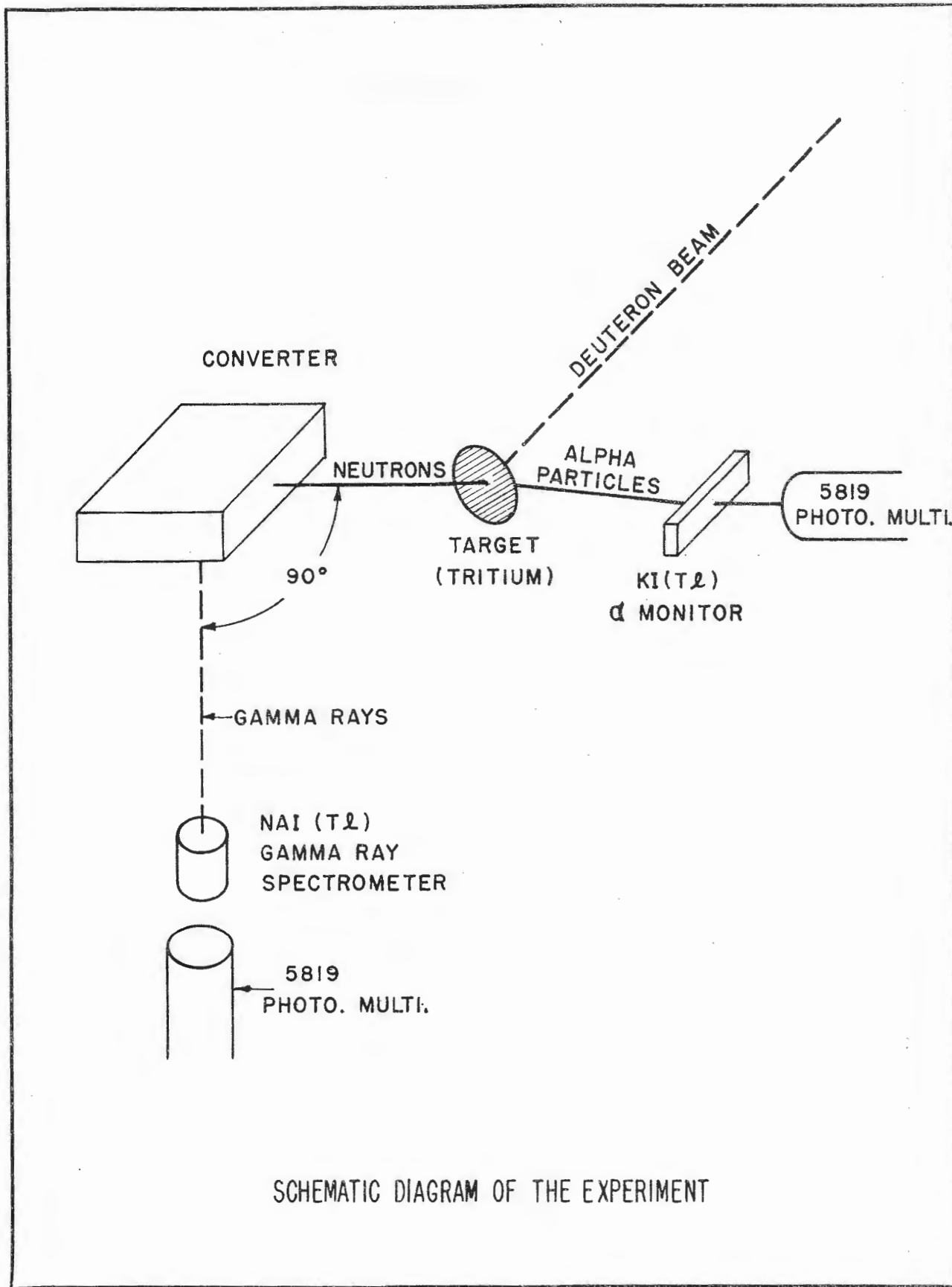
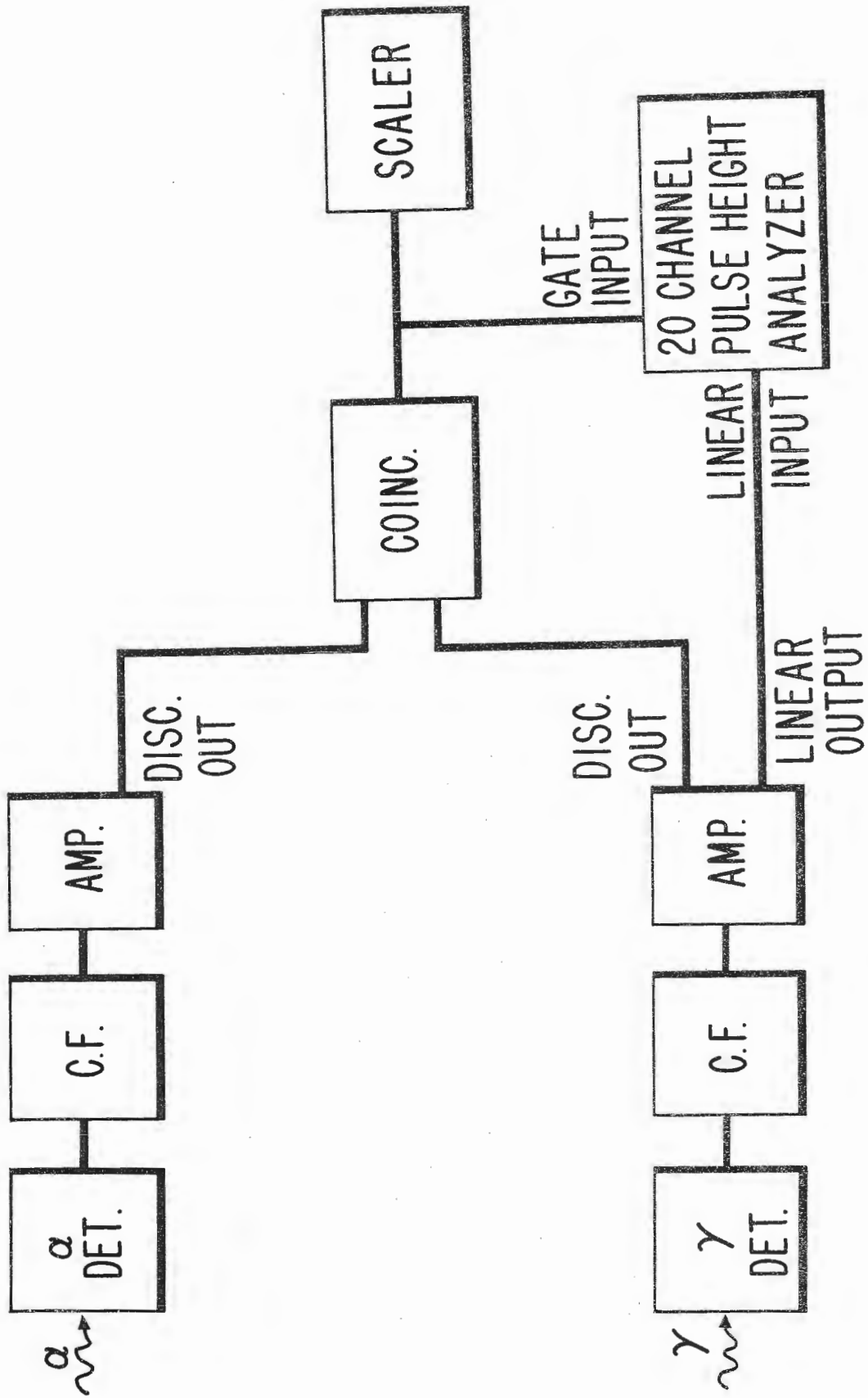


FIGURE 1 SCHEMATIC DIAGRAM OF THE EXPERIMENT.



BLOCK DIAGRAM OF ELECTRONICS

FIGURE 2 BLOCK DIAGRAM OF THE ELECTRONIC ARRANGEMENT.

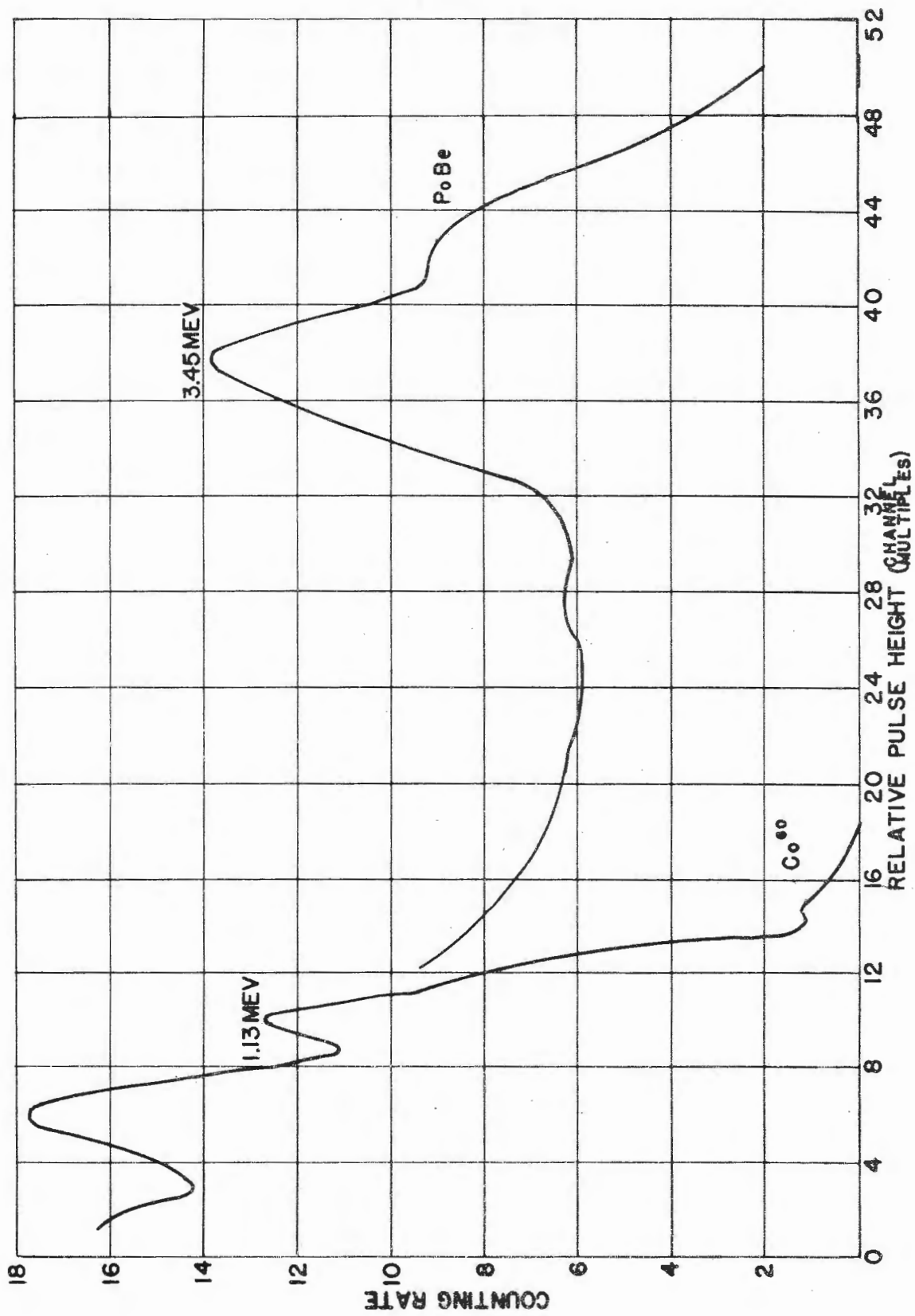


FIGURE 3 TYPICAL ENERGY CALIBRATION CURVES OF THE SINGLE CRYSTAL SPECTROMETER.

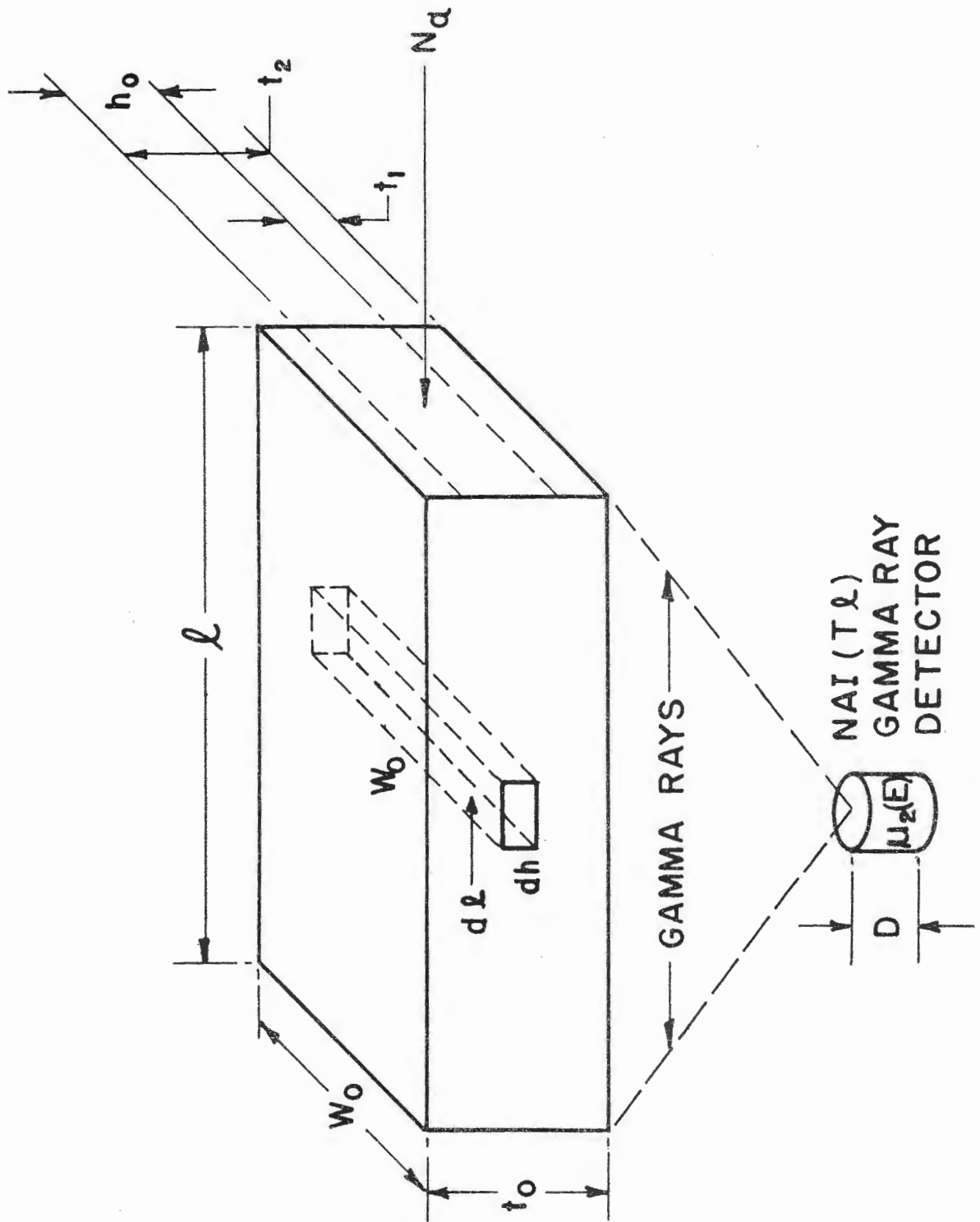


FIGURE 4 GEOMETRICAL ARRANGEMENT OF CONVERTER AND SPECTROMETER CRYSTALS.

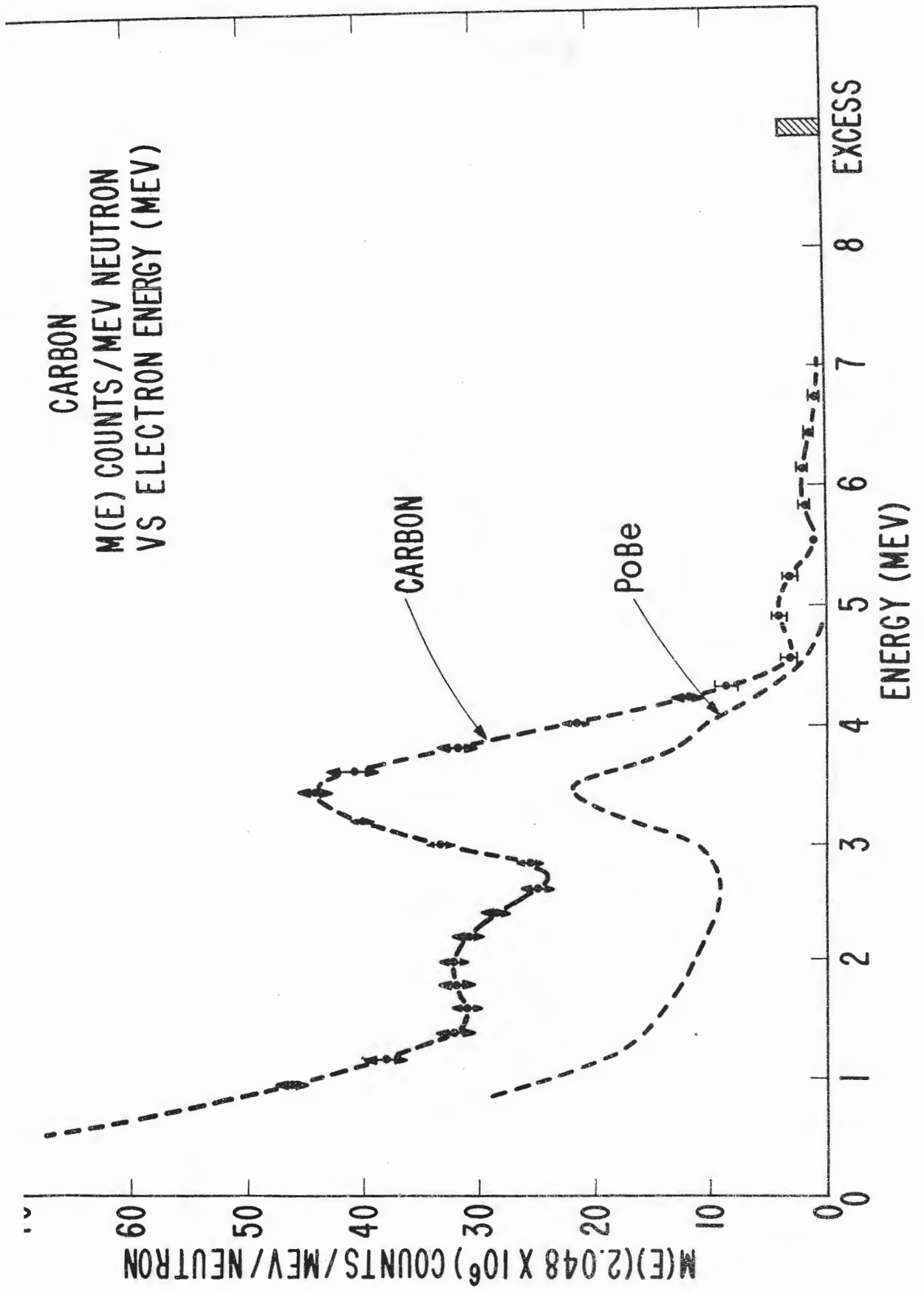


FIGURE 5 PULSE HEIGHT DISTRIBUTION OF CARBON GAMMA RAYS.

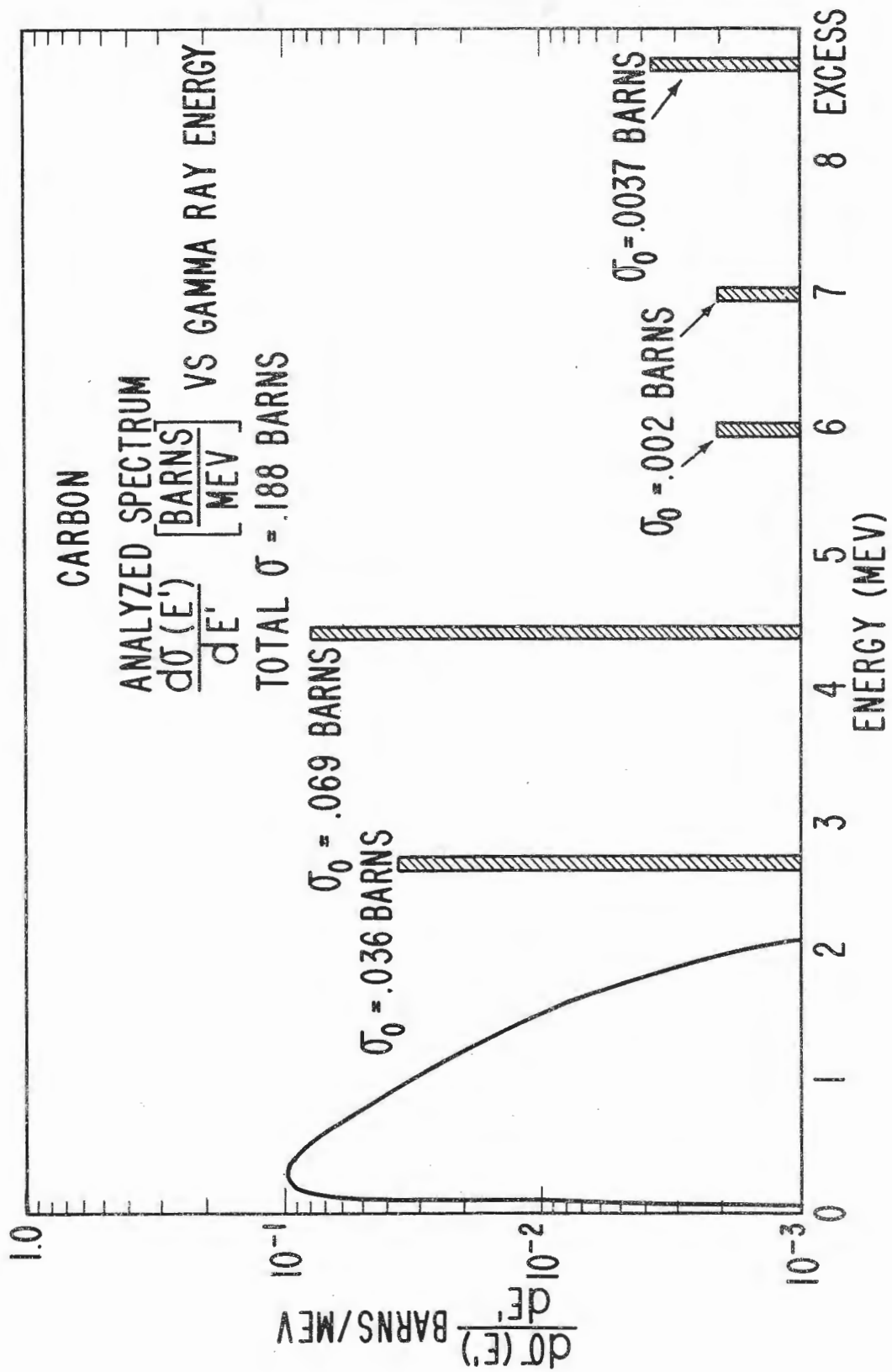


FIGURE 6 SPECTRAL DISTRIBUTION OF CARBON GAMMA RAYS.

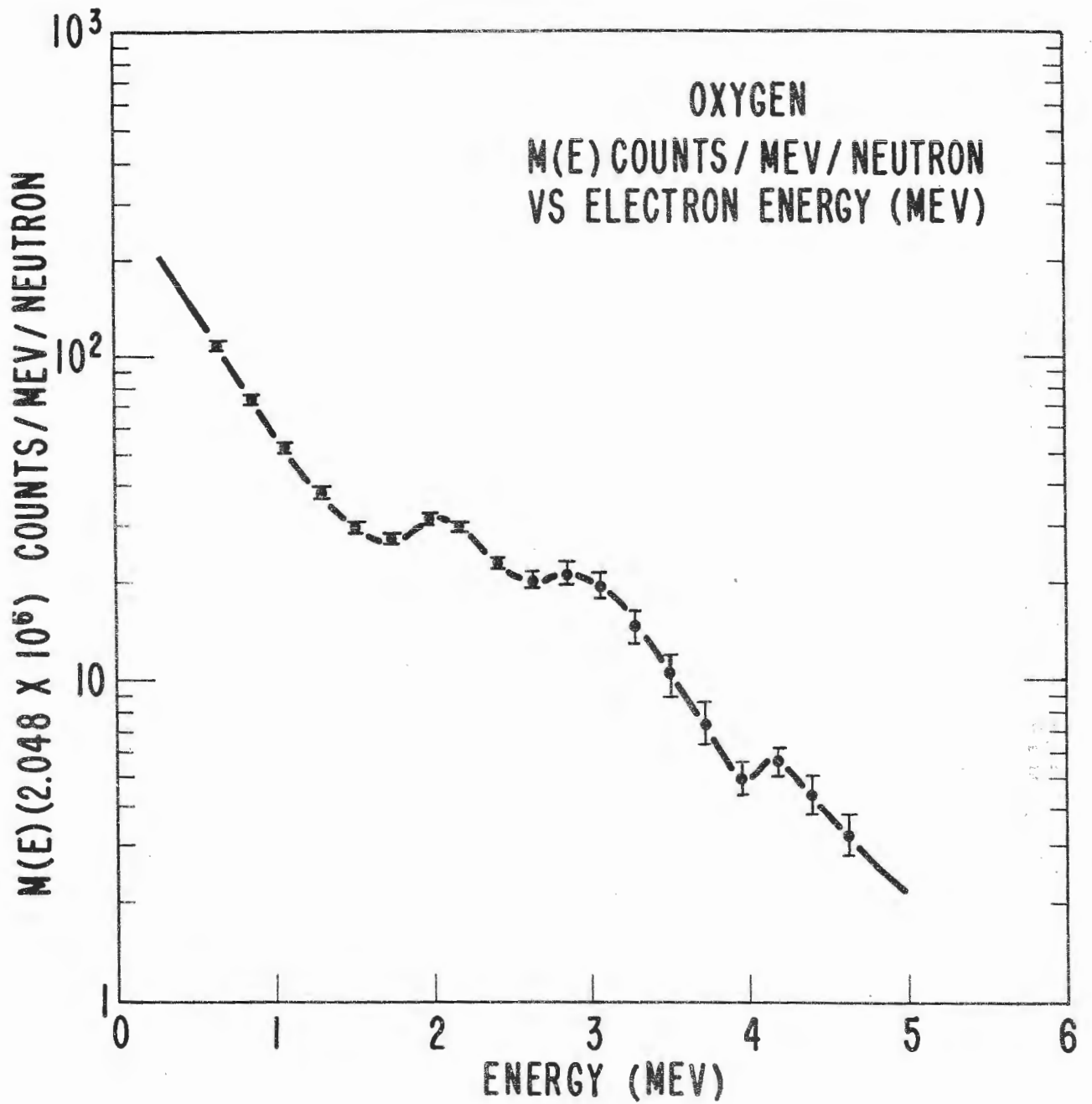


FIGURE 7 PULSE HEIGHT DISTRIBUTION OF OXYGEN GAMMA RAYS.

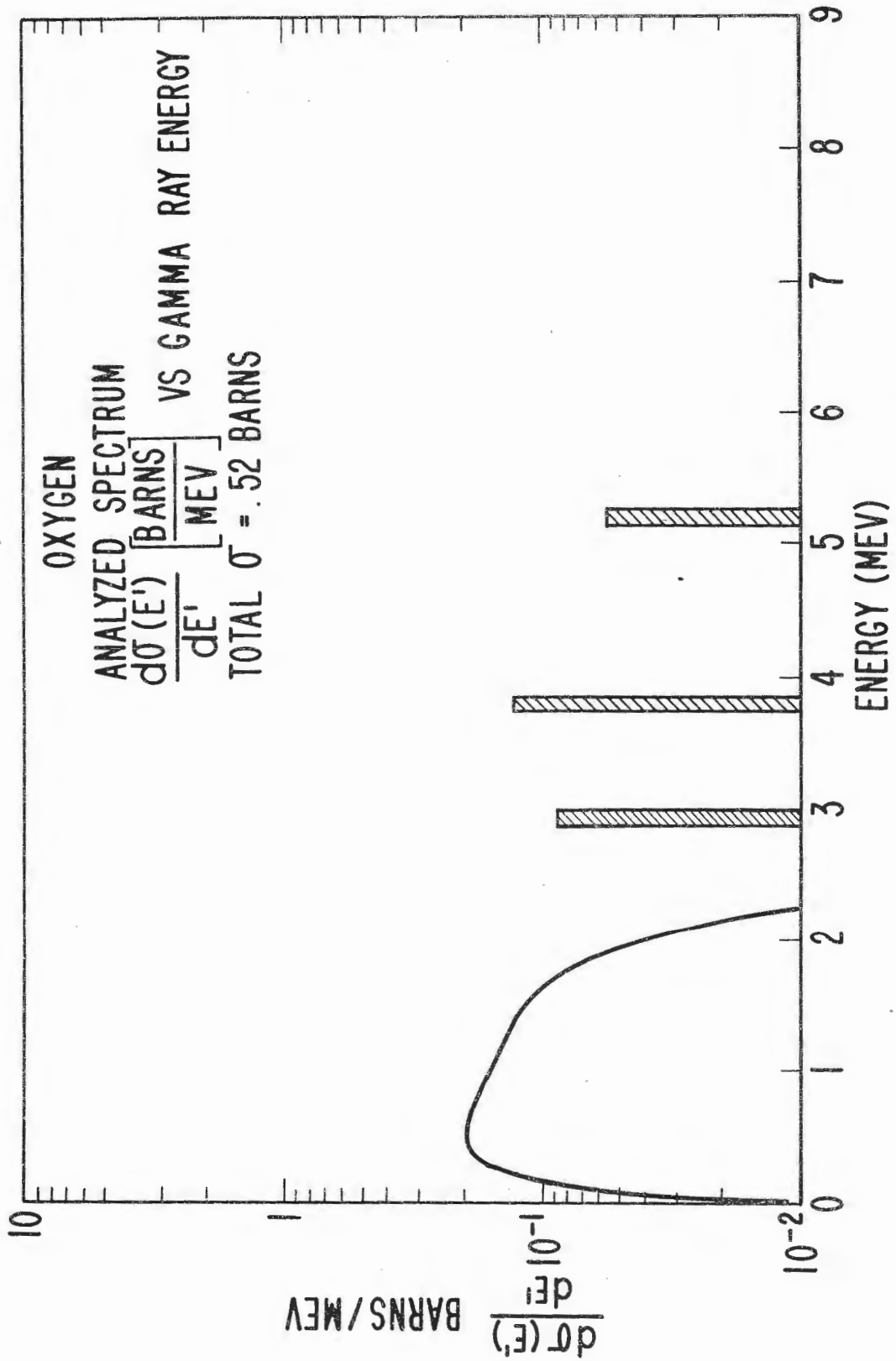
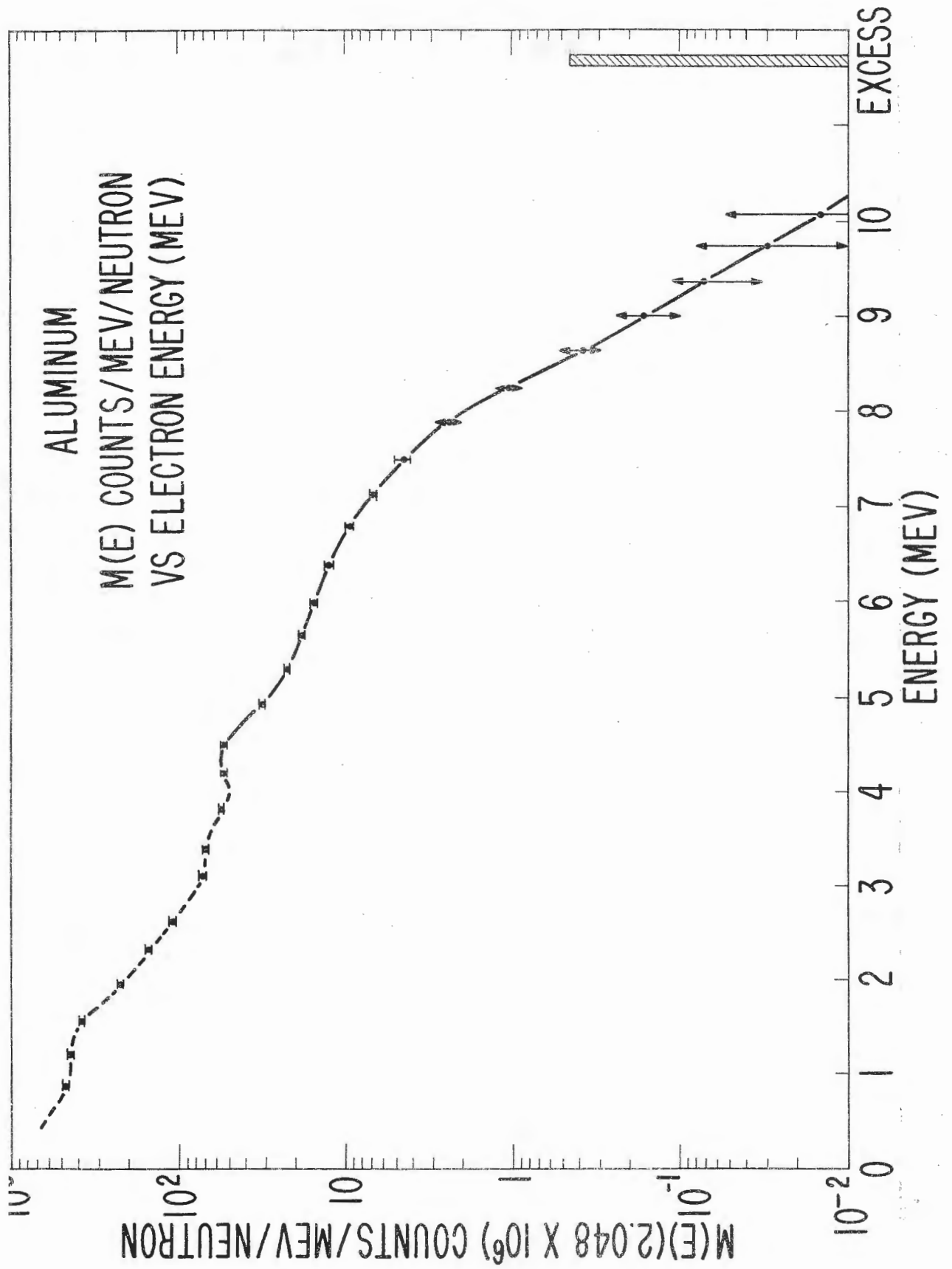


FIGURE 8 SPECTRAL DISTRIBUTION OF OXYGEN GAMMA RAYS.



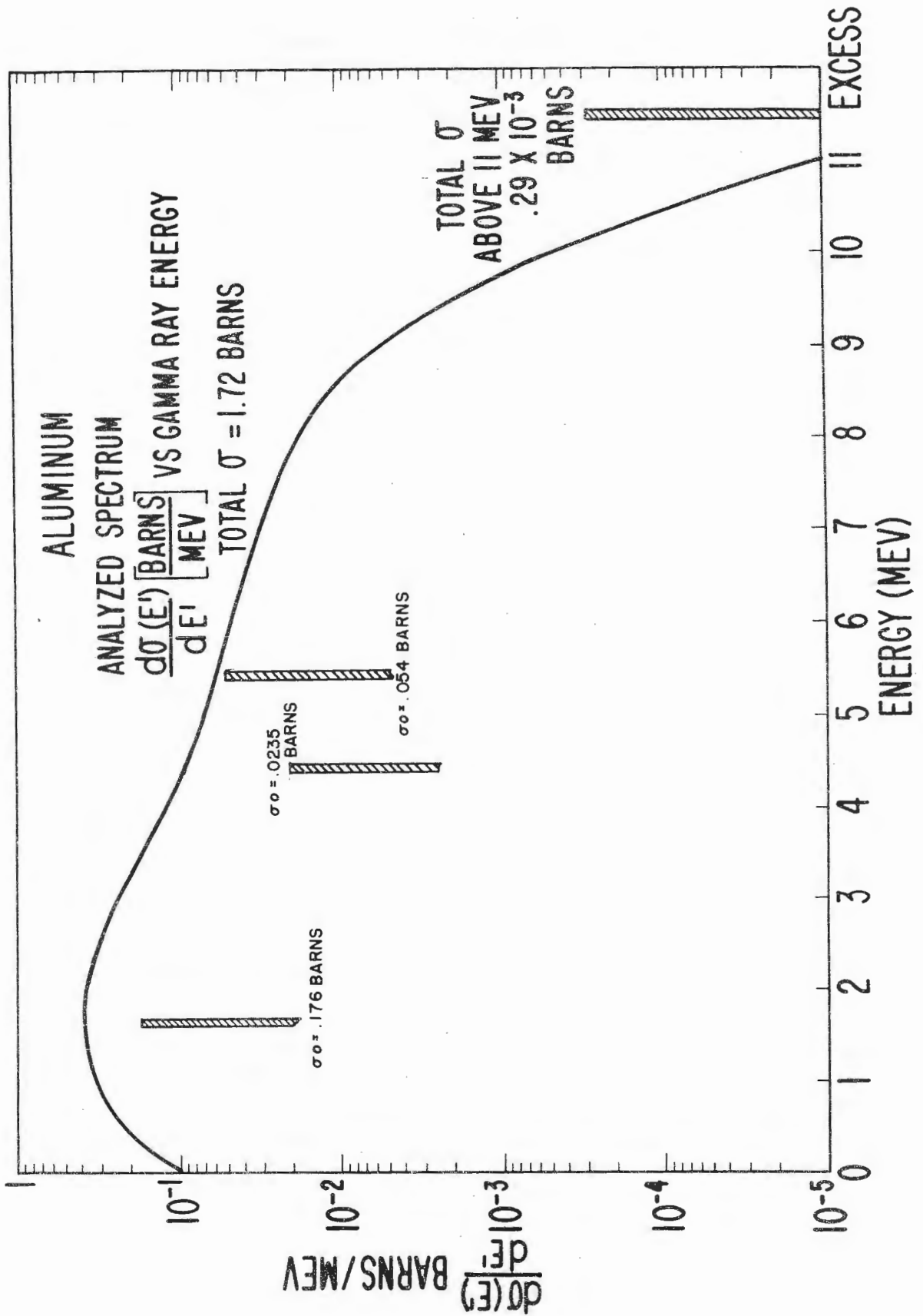


FIGURE 10 SPECTRAL DISTRIBUTION OF ALUMINUM GAMMA RAYS.

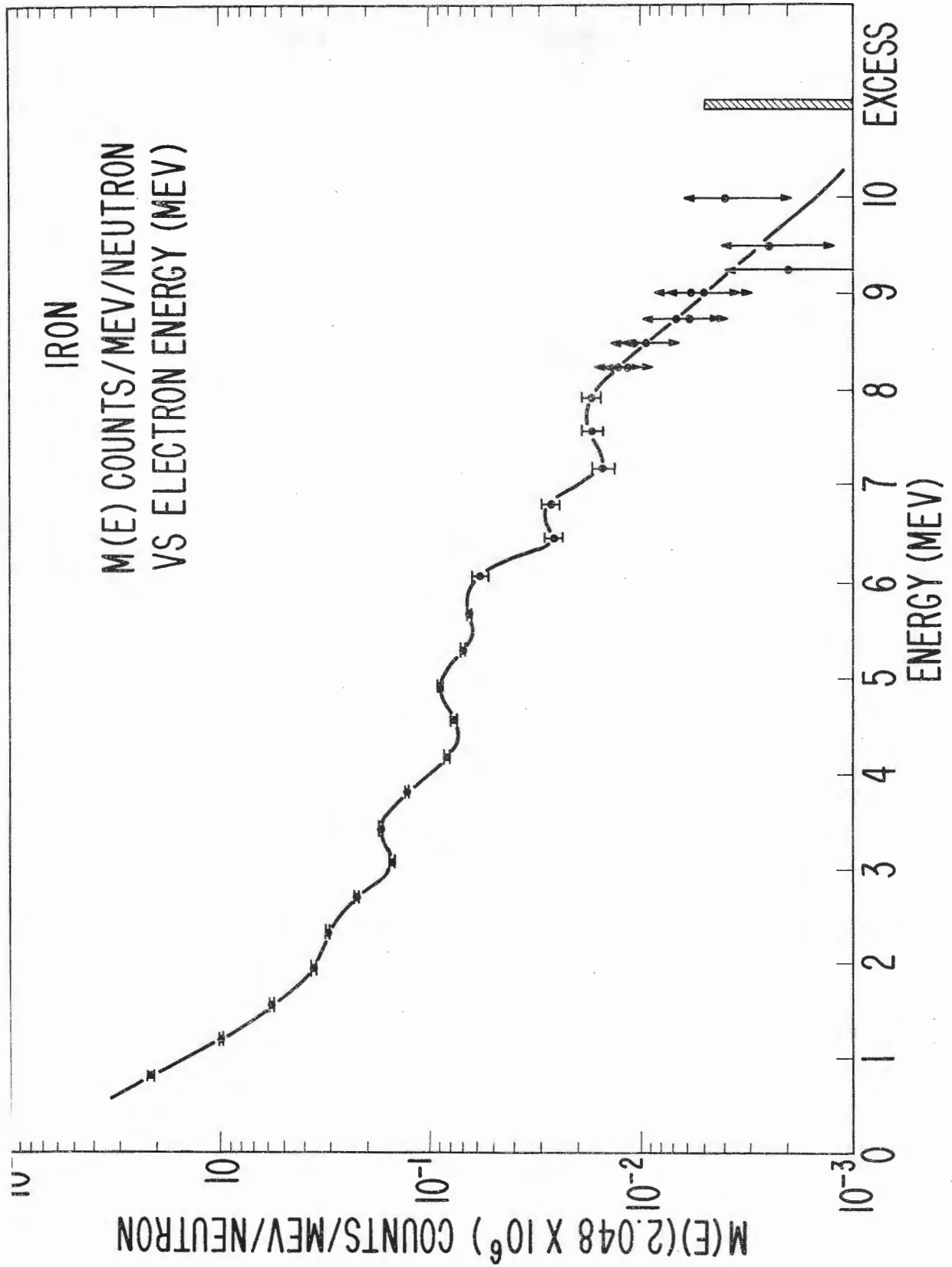


FIGURE 11 PULSE HEIGHT DISTRIBUTION OF IRON GAMMA RAYS.

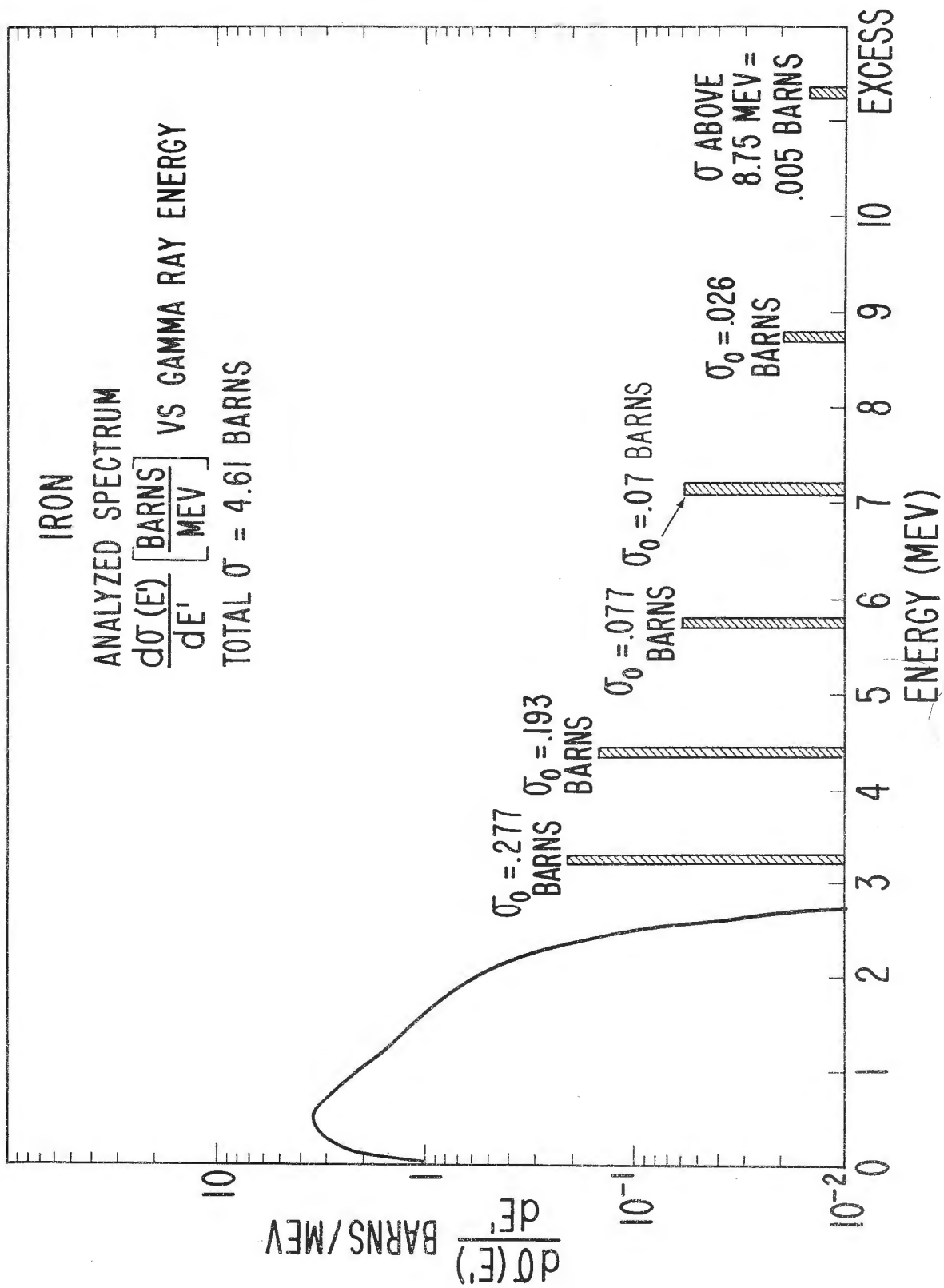
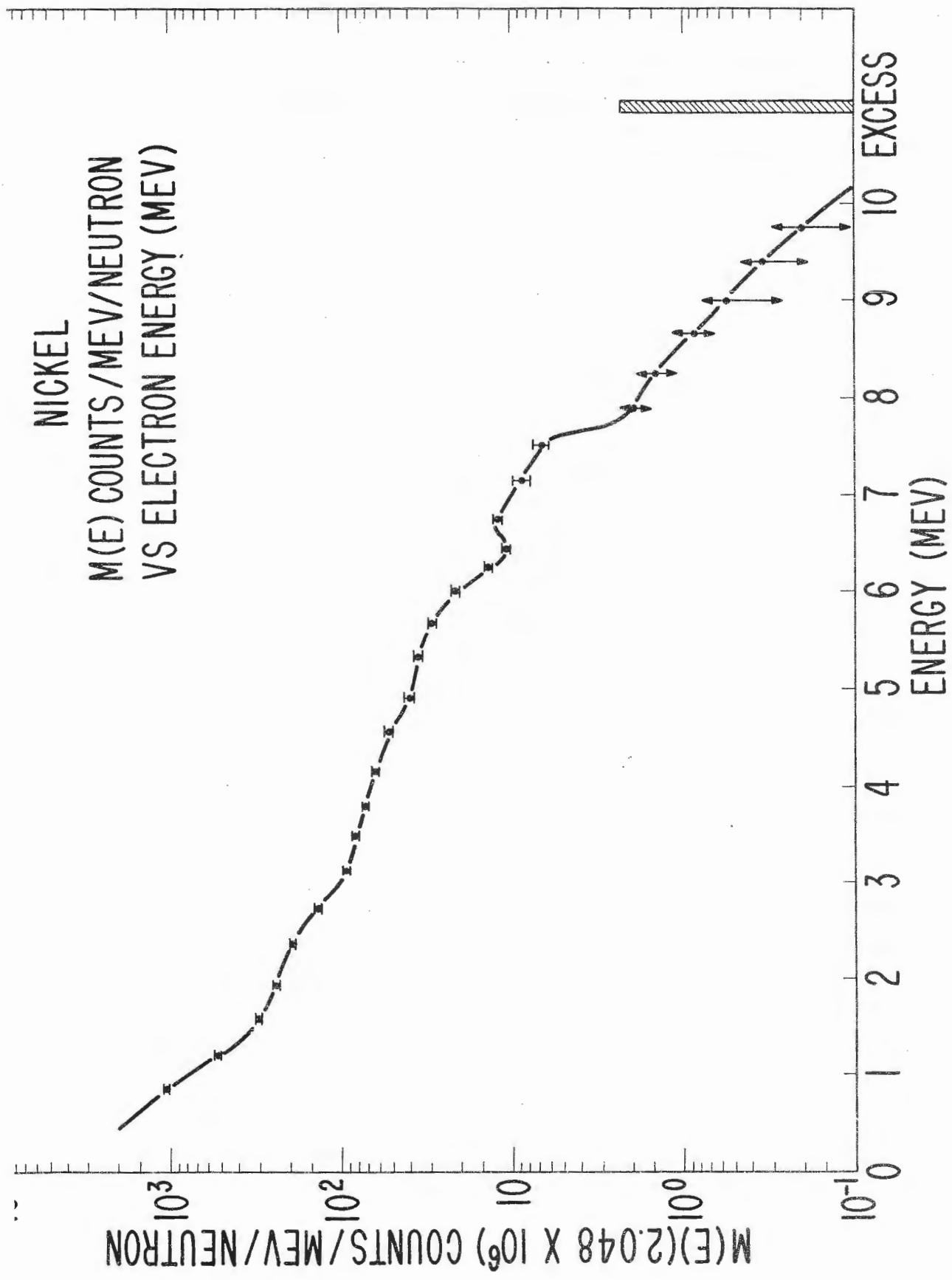


FIGURE 12 SPECTRAL DISTRIBUTION OF IRON GAMMA RAYS.



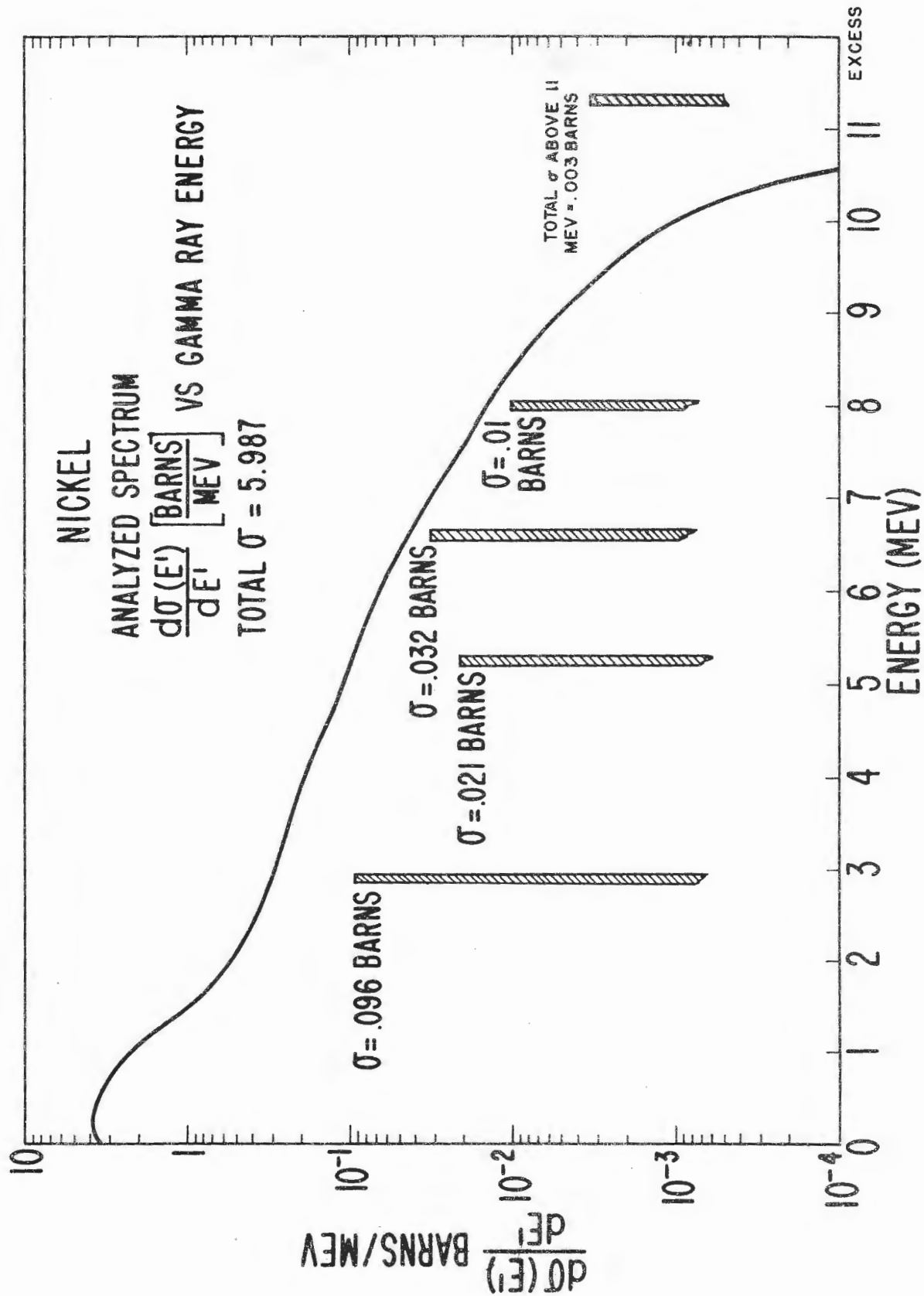
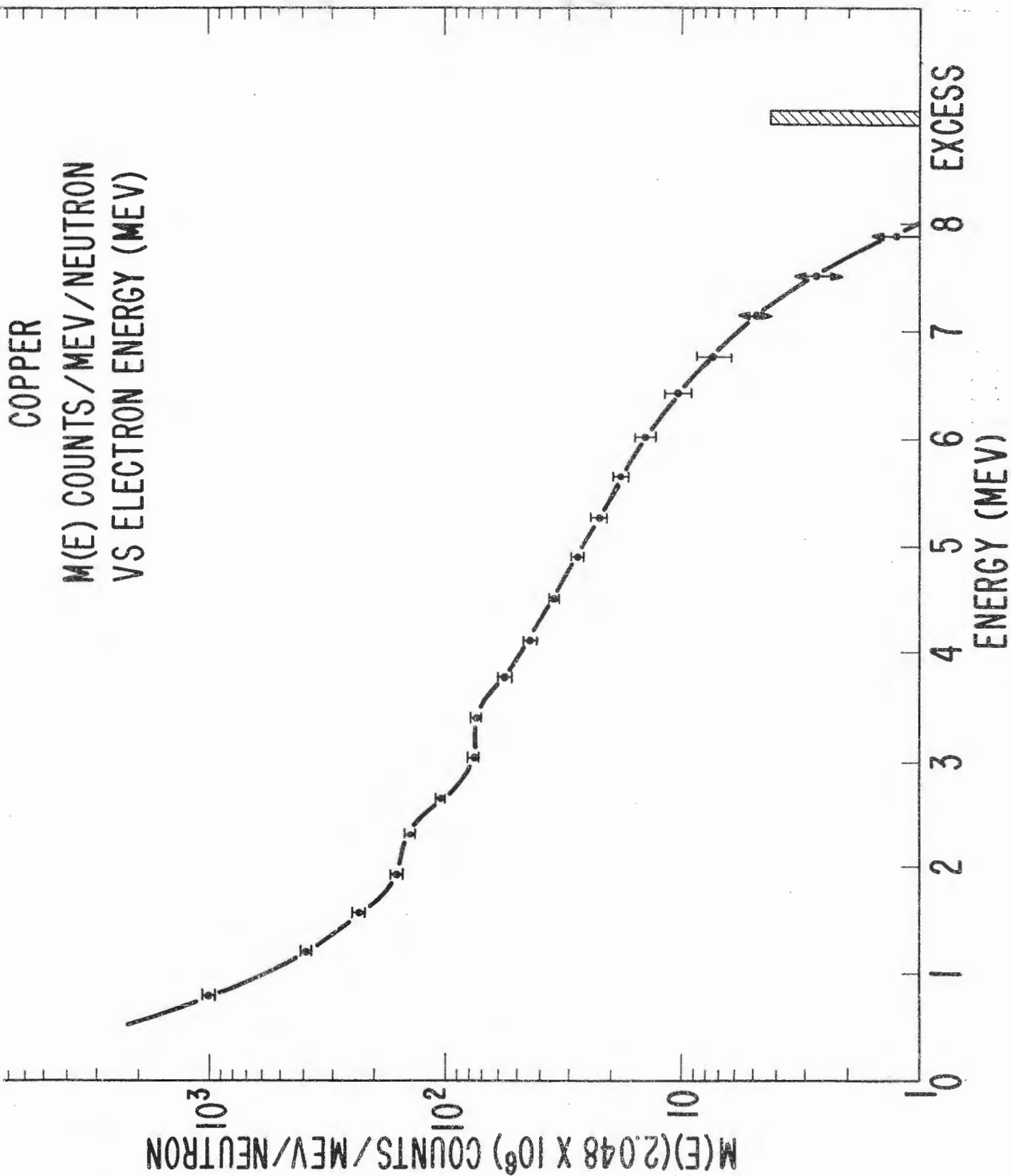


FIGURE 14 SPECTRAL DISTRIBUTION OF NICKEL GAMMA RAYS.



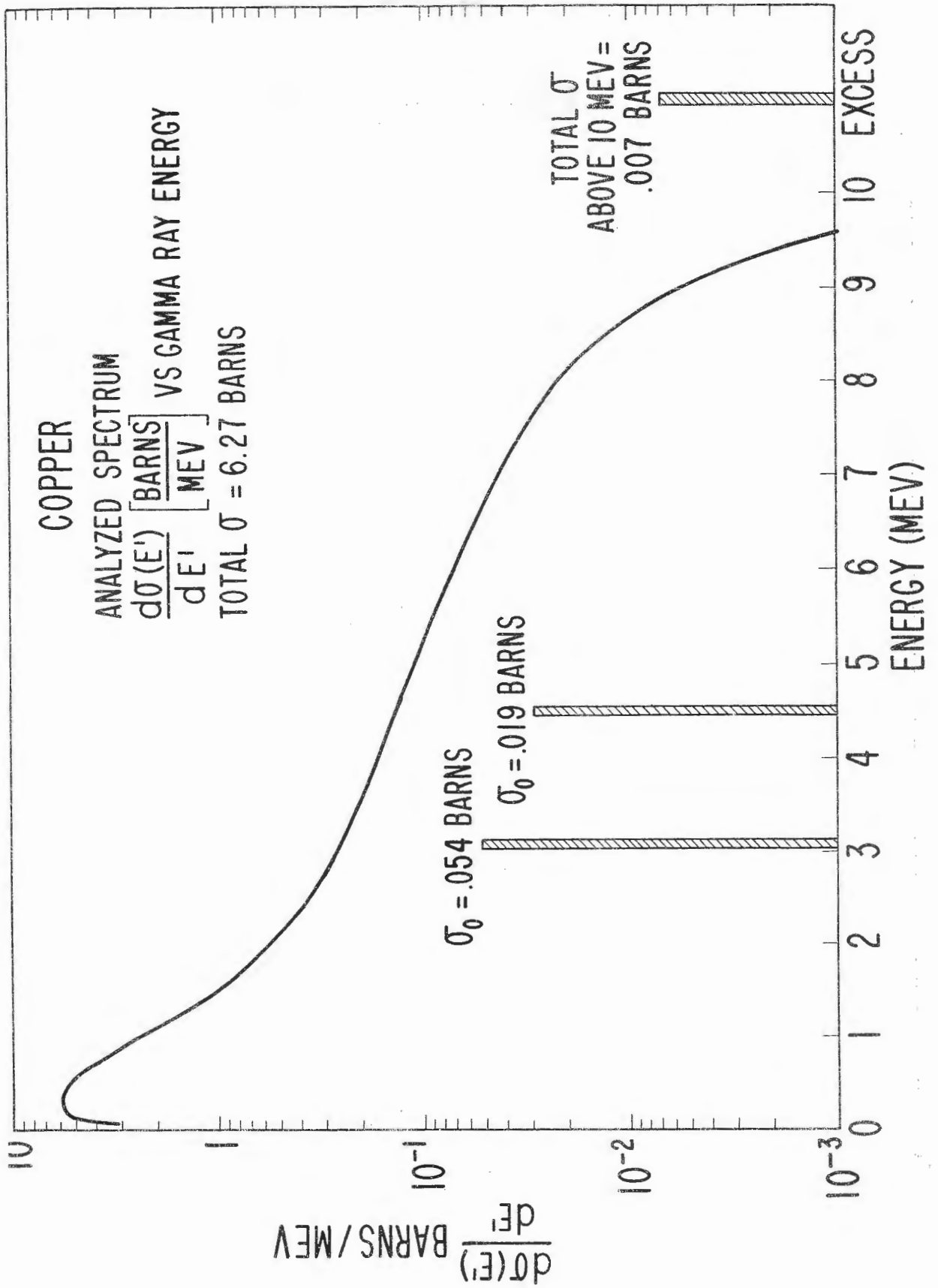


FIGURE 16 SPECTRAL DISTRIBUTION OF COPPER GAMMA RAYS.

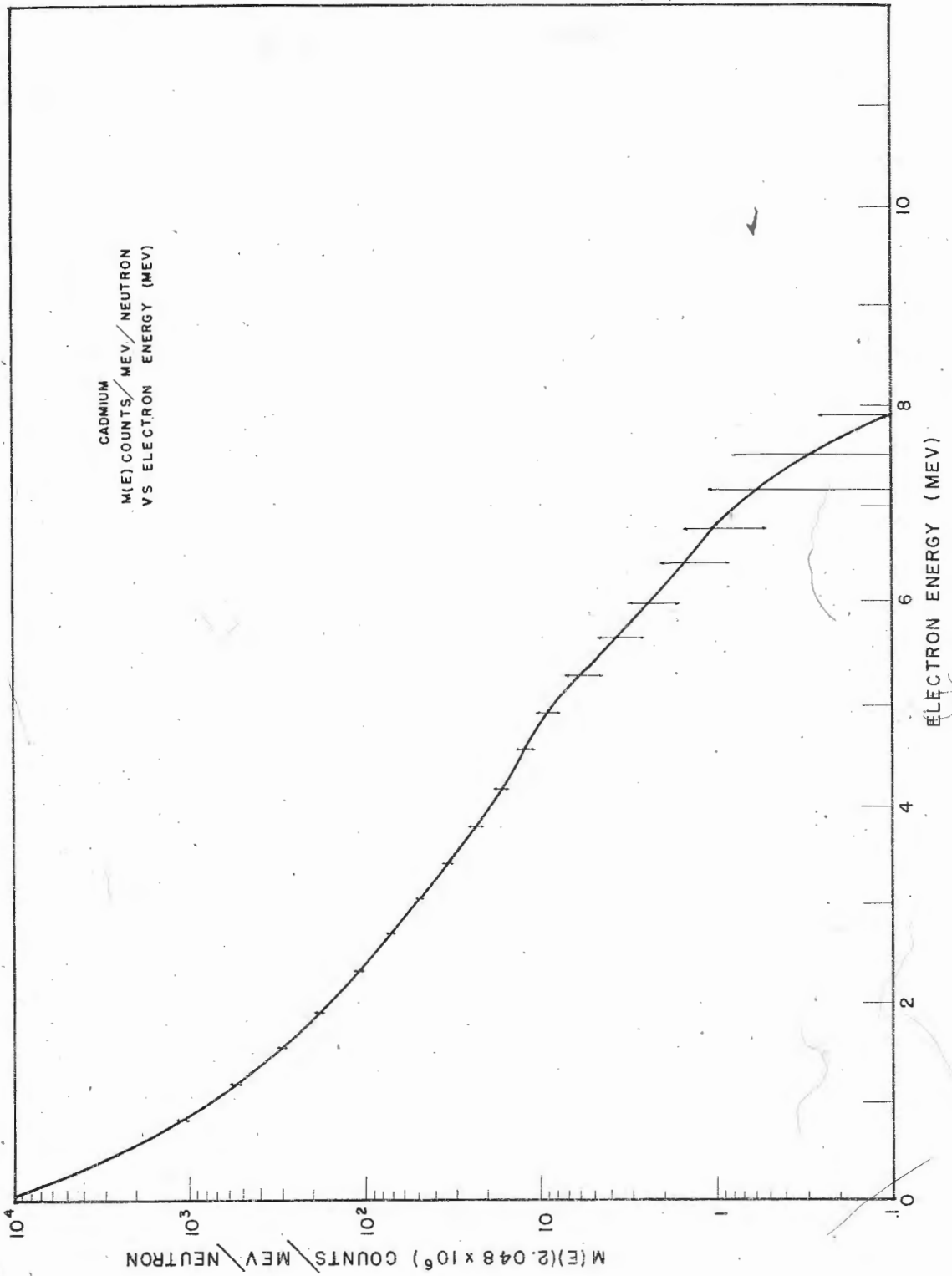


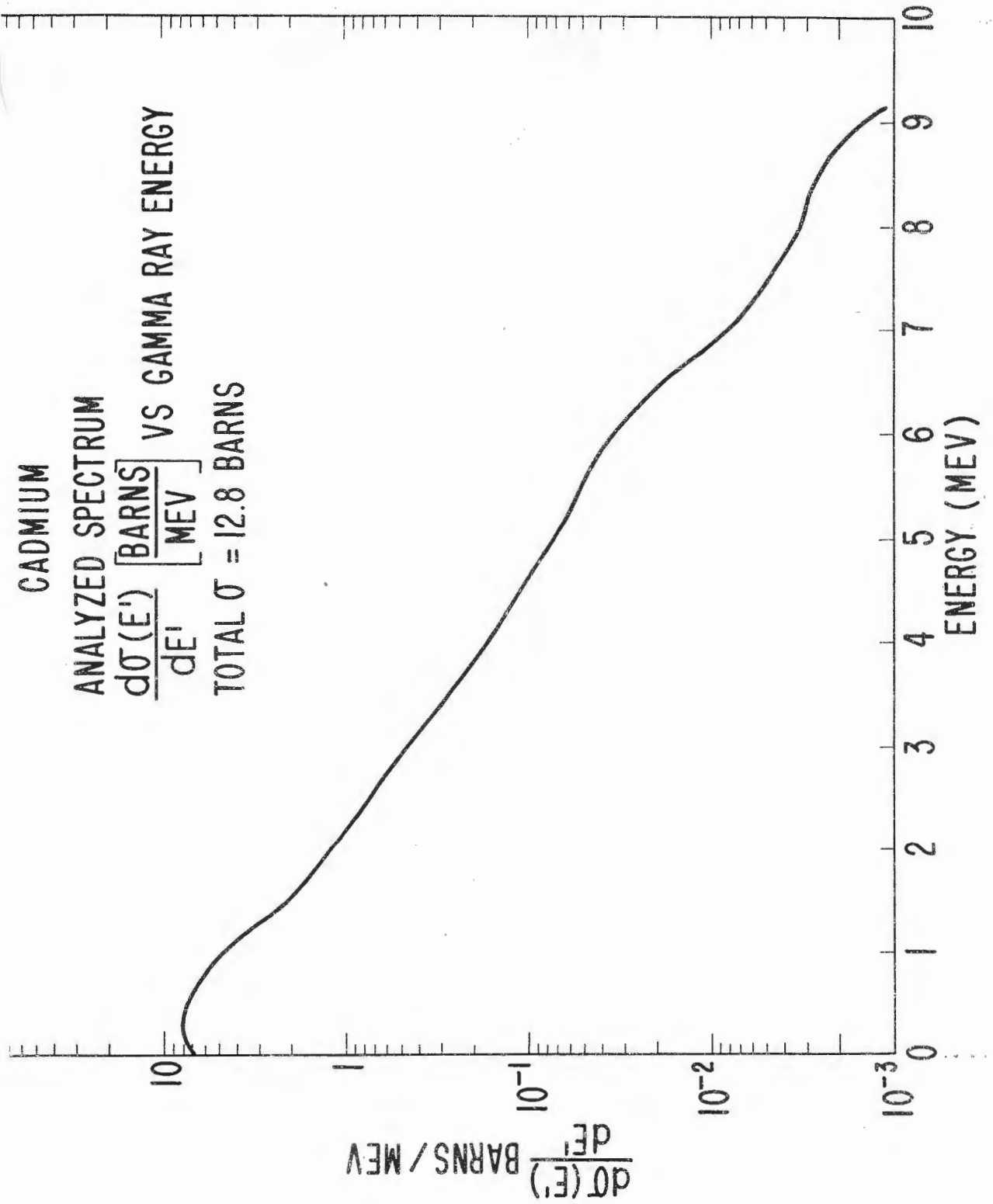
FIGURE 17 PULSE HEIGHT DISTRIBUTION OF CADMIUM GAMMA RAYS.

CADMIUM

ANALYZED SPECTRUM

$\frac{d\sigma(E')}{dE'} \left[ \frac{\text{BARN}}{\text{MEV}} \right]$  VS GAMMA RAY ENERGY

TOTAL  $\sigma = 12.8$  BARN



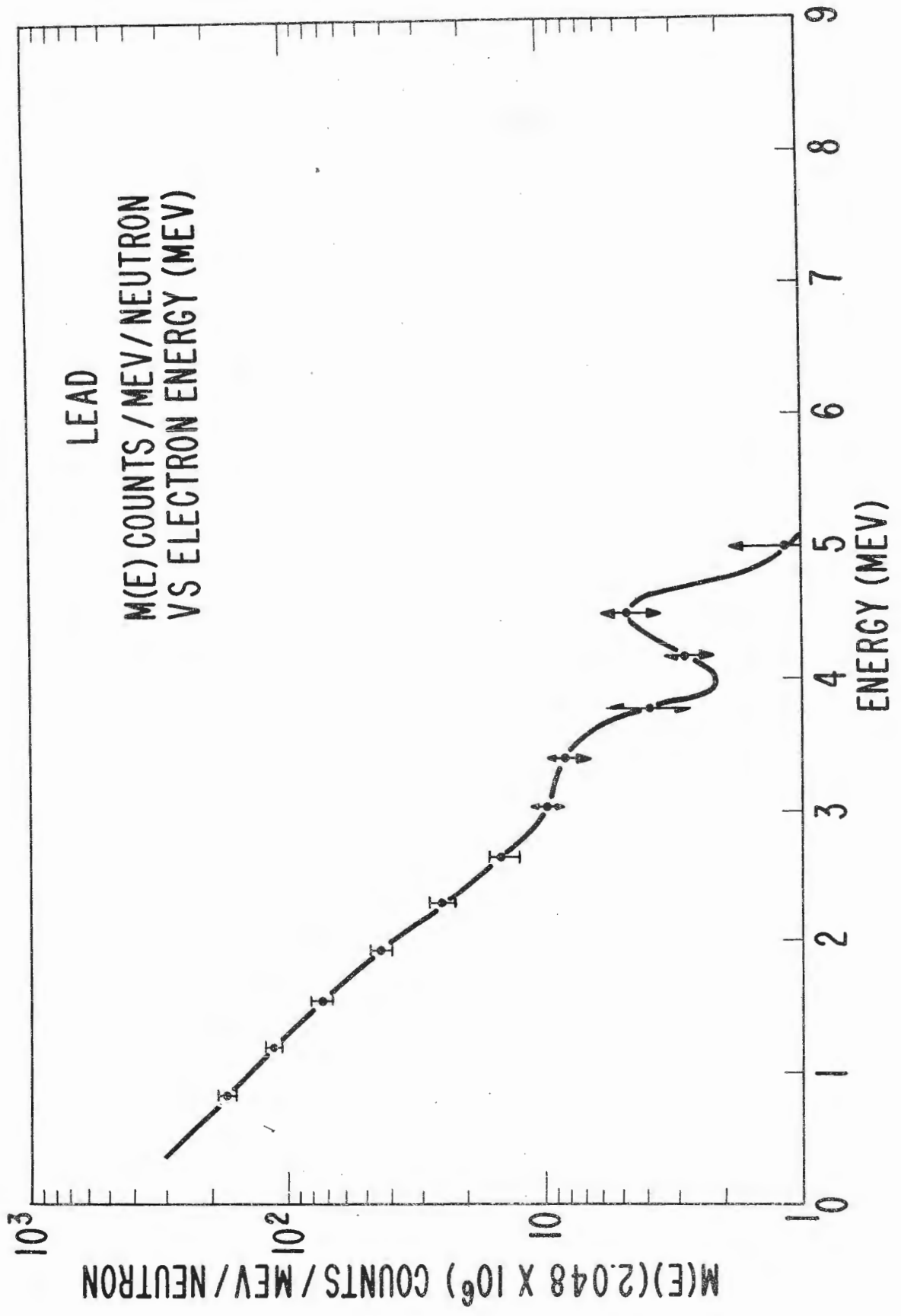


FIGURE 19 PULSE HEIGHT DISTRIBUTION OF LEAD GAMMA RAYS.

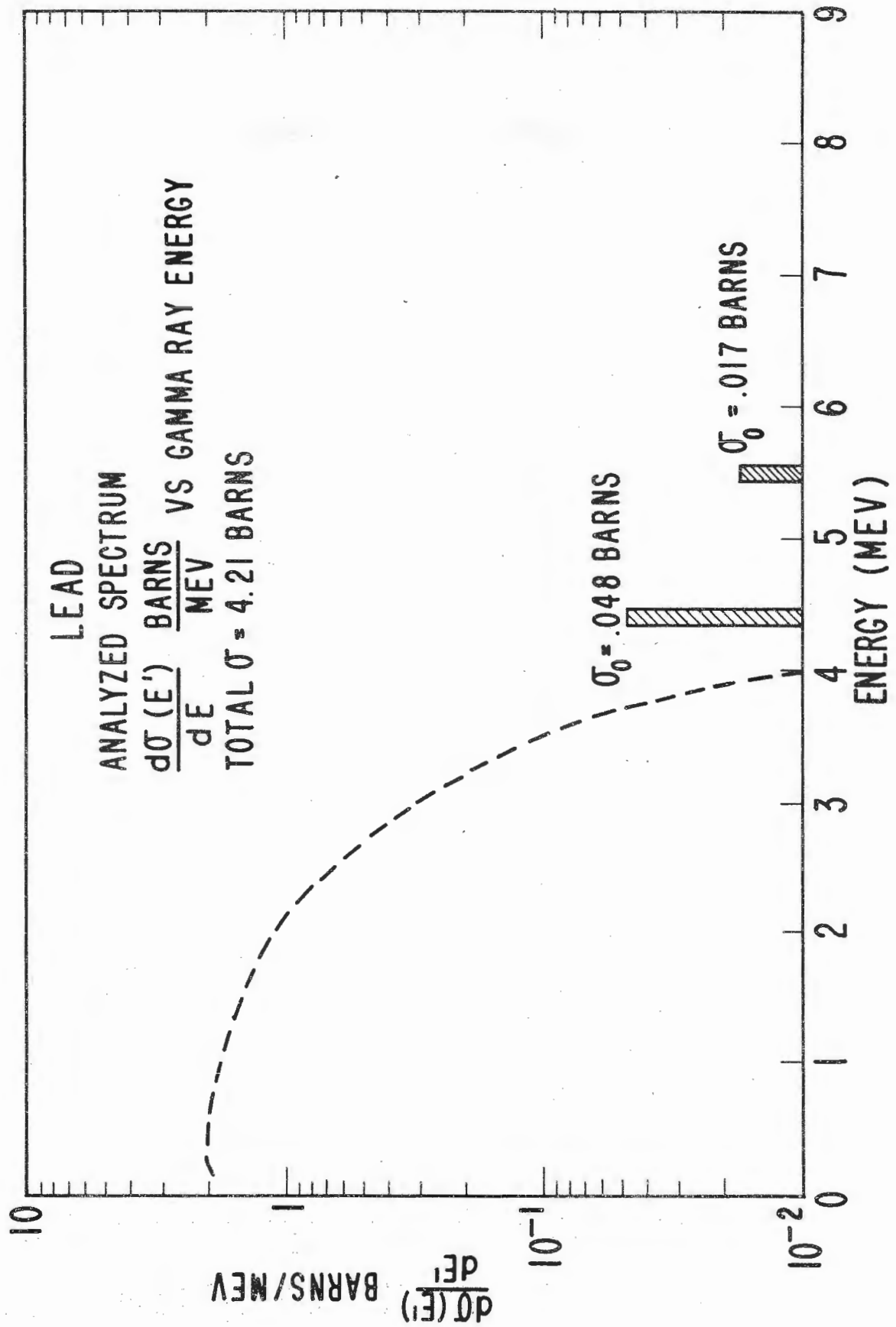


FIGURE 20 SPECTRAL DISTRIBUTION OF LEAD GAMMA RAYS.

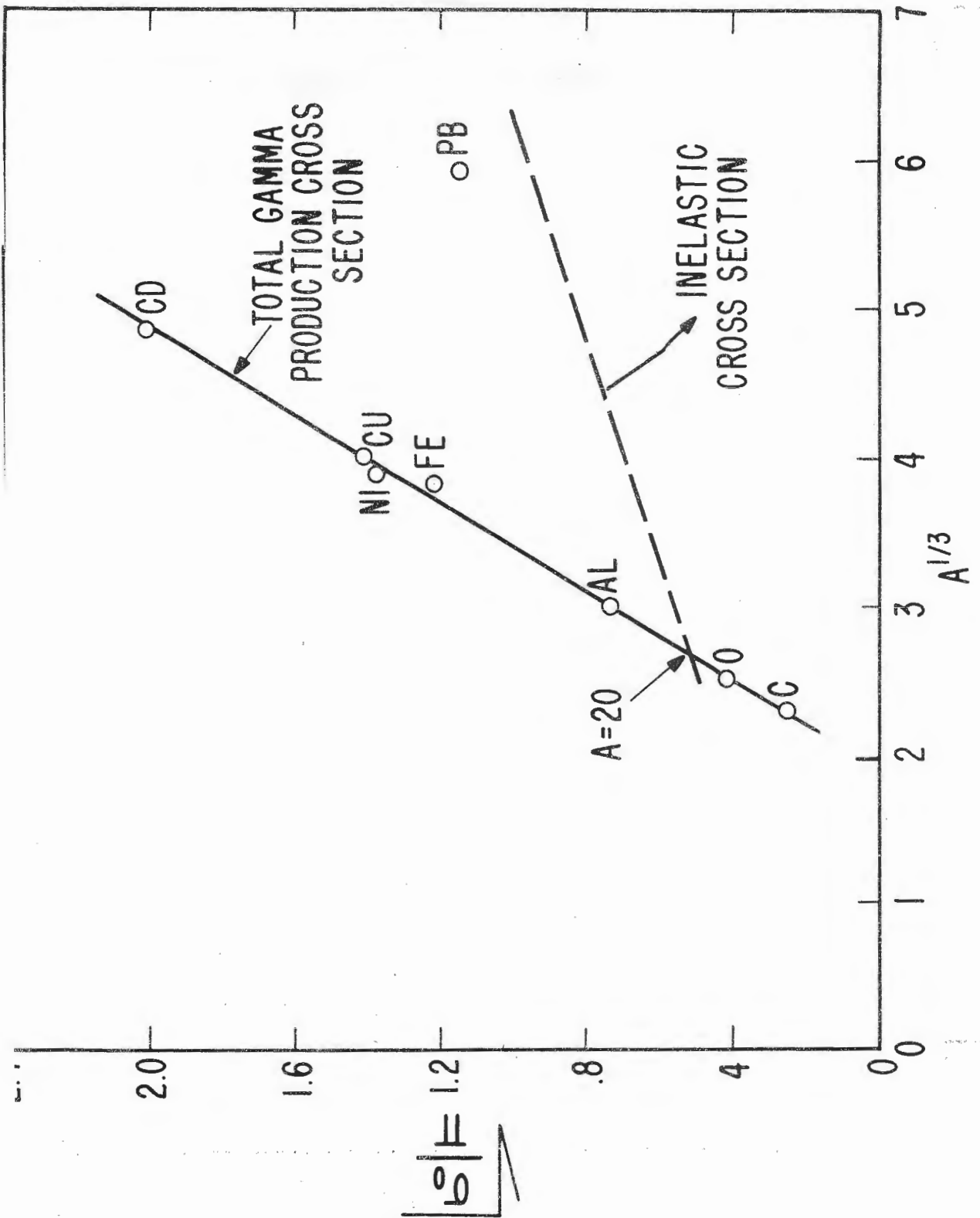


FIGURE 21 GAMMA RAY PRODUCTION CROSS SECTION SHOWN AS A